

# Subcarrier Grouping-Enabled Improvement in Transmission Performance of Subcarrier Index-Power Modulated Optical OFDM for IM/DD PON Systems

Al Halabi, Fadi; Chen, Lin; Giddings, Roger; Hamie, Ali; Tang, Jianming

**Journal of Lightwave Technology**

*DOI:*
10.1109/JLT.2018.2863751

Published: 15/10/2018

Peer reviewed version

# Subcarrier Grouping-enabled Improvement in Transmission Performance of Subcarrier Index-Power Modulated Optical OFDM for IM/DD PON Systems

F. Halabi, L. Chen, R. P. Giddings, A. Hamié, and J. M. Tang

***Abstract*— As an improved variant of a previously published subcarrier index-power modulated optical orthogonal frequency division multiplexing (SIPM-OOFDM), a signal transmission technique termed subcarrier index-power modulated OOFDM with subcarrier grouping (SIPM-SG-OOFDM) is proposed and investigated for the first time. In SIPM-SG-OOFDM, each symbol is divided into multiple subcarrier groups, each of which is assigned with a specific power pattern according to an incoming data sequence. As such, in comparison with conventional OOFDM, extra information bits are conveyed without significantly compromising the transceiver complexity. In addition, subcarrier grouping also offers highly desired zero-overhead automatic error correction at the receiver. Detailed analysis and numerical simulations are undertaken to identify optimum SIPM-SG-OOFDM transceiver parameters and also to explore the corresponding maximum achievable transmission performances over passive optical network systems based on intensity-modulation and direct-detection. It is shown that, compared to SIPM-OOFDM, SIPM-SG-OOFDM not only increases the signal transmission capacity by 11% but also improves the system power budget by approximately 1.0dB.**

***Index Terms*— Optical orthogonal frequency division multiplexing, signal modulation and passive optical networks.**

## I. Introduction

MULTICARRIER modulation (MCM) is considered to be a key enabling technique for use in fading dispersive optical communications systems due to its large signal transmission capacity, excellent adaptability to system impairments, good flexibility and reconfigurability, as well as relatively high cost-effectiveness [1]. As one of the most widely researched MCM techniques, over the past ten years, optical orthogonal frequency division multiplexing (OOFDM) has gained overwhelming attention in the optical communication research and development (R&D) community, as OOFDM is equipped with additional highly desired features such as software-controllable optimum trade-offs among the following parameters: achievable signal transmission capacity, spectral efficiency and transceiver complexity [2]-[5]. For a wide diversity of cost-sensitive application scenarios, such a feature is greatly advantageous for producing versatile OOFDM transceivers with effectively reduced transceiver costs without considerably compromising their system performances.

The past decade has seen persistent research effort made to further enhance signal transmission capacities of OOFDM transmission systems. As a direct result, a large number of technical approaches have been proposed, including polarization division multiplexing (PDM) [6], code division multiplexing (CDM) [7] and wavelength division multiplexing (WDM) [8]. However, the aforementioned straightforward multiplexing approaches often require expensive optical components and sophisticated and bulky transceiver architectures. Unavoidably, this is prohibitive for its practical implementation in cost-sensitive passive optical networks (PONs). Therefore, it is extremely beneficial that full use is made of digital signal processing (DSP) to introduce an extra information-bearing dimension in OOFDM without requiring any additional analogue optical/electrical hardware.

In addition to optical transmission systems, a very similar open question has also been recently raised by the wireless communications R&D community. To address the technical challenge associated with wireless transmission systems, subcarrier index modulated OFDM (SIM-OFDM) has been proposed, in which subcarrier index is exploited as an extra information-bearing dimension to carry user information. Specifically, in SIM-OFDM a subcarrier is activated or deactivated according to the incoming data sequence, thus the resulting on-and-off subcarrier power pattern within each individual OFDM symbol also bears user information. However, compared to conventional OFDM, SIM-OFDM has to divvy up the achievable signal transmission capacity and spectral efficiency, because almost half of the subcarriers are deactivated. In addition, the incorrect detection of a subcarrier power status at the receiver also causes the error propagation effect to occur [9]. To solve such an error propagation issue, OFDM with index modulation (OFDM-IM) has been reported in [10], where both transmitter subcarrier power status-mapping and receiver log-likelihood ratio detection are implemented to determine the most likely active subcarriers. It is clear that, very similar to SIM-OFDM, not all subcarriers in OFDM-IM are active, hence OFDM-IM still suffers the unwanted large reductions in both signal transmission capacity and spectral efficiency. Furthermore, the DSP complexity of the OFDM-IM detector grows exponentially with increasing subcarrier counts, this may considerably constrain its practical application.

F. Halabi, R. P. Giddings, and J. M. Tang are with the School of Electrical Engineering, Bangor University, Bangor LL57 1UT, U.K. (e-mails: eep604@bangor.ac.uk; r.p.giddings@bangor.ac.uk; j.tang@bangor.ac.uk).

L. Chen is with the College of Electronics and Information Engineering, Shanghai University of Electric Power, Shanghai, 200090, China. (e-mail: l.chen@bangor.ac.uk)

A. Hamié is with the CRITC Lab, Arts, Sciences and Technology University in Lebanon University, Beirut 1102 2801, Lebanon (e-mail: ali.hamie@aul.edu.lb).

To address the abovementioned technical challenges associated with both SIM-OFDM and OFDM-IM, and also to explore cost-effective solutions for PON application scenarios, very recently subcarrier index-power modulated optical OFDM (SIPM-OOFDM) has been reported [11], in which both the subcarrier index and subcarrier power jointly acts as an extra information-carrying dimension, referred to as subcarrier index-power (SIP) information-bearing dimension throughout this paper. In SIPM-OOFDM, each individual subcarrier is set at a low or high power level according to the incoming data sequence, and the high and low power subcarriers are encoded with 8-phase shift keying (8-PSK) and quadrature-phase shift keying (QPSK), respectively. Such an encoding procedure ensures that all the subcarriers are active and also, compared to conventional OFDM, enables one extra information bit to be conveyed per subcarrier in the SIP information-bearing dimension. More recently, SIPM-OOFDM with superposition multiplexing (SIPM-OOFDM-SPM) [12] has also been published, in which superposition multiplexing passively adds two complex numbers together: one encoded with 8-PSK and the other with QPSK, and the resulting sum is then assigned to high power subcarriers only, whilst low power subcarriers are still encoded using QPSK. Therefore, in comparison with SIPM-OOFDM, SIPM-OOFDM-SPM enables the more effective usage of all high power subcarriers and thus a further 28.6% increase in signal transmission capacity is obtainable. Most recently, an improved variant of both SIPM-OOFDM and SIPM-OOFDM-SPM, known as multilevel subcarrier index-power modulated optical OFDM (ML-SIPM-OOFDM) has also been reported in [13]. In ML-SIPM-OOFDM, four subcarrier power levels are introduced to allow each subcarrier to carry two extra information bits in the SIP information-bearing dimension. It is worth mentioning that in all these three previously published techniques, namely SIPM-OOFDM, SIPM-OOFDM-SPM and ML-SIPM-OOFDM, no physical mechanisms have been introduced to automatically correct errors at the receiver.

In this paper, we propose, for the first time, a significantly improved variant of SIPM-OOFDM, termed subcarrier index power modulated optical OFDM with subcarrier grouping (SIPM-SG-OOFDM). Similar to SIPM-OOFDM, in SIPM-SG-OOFDM all the 8-PSK/QPSK-encoded subcarriers of two power levels are kept active, and each individual symbol is divided into multiple subcarrier groups having specifically been assigned subcarrier power patterns. According to the incoming data sequence, the subcarrier power pattern within each subcarrier group is selected from a predefined subcarrier power pattern set. This allows each subcarrier group to bear extra user information bits. For simplicity, throughout the paper we refer to this dimension as subcarrier group (SG) information-bearing dimension. Compared to SIPM-OOFDM encoded using the same modulation formats, SIPM-SG-OOFDM offers an increase in signal bit rate by approximately 11%. In addition, subcarrier grouping also provides SIPM-SG-OOFDM with an additional capability of automatically detecting and subsequently correcting SG information-bearing dimension errors at the receiver without consuming any valuable transmission bandwidth. As a direct result of the zero-overhead error correction capability, the abovementioned signal transmission capacity improvement is also companied with a 1dB gain in optical signal to noise ratio (OSNR) in intensity-modulation and direct-detection (IM/DD) 25km standard single-mode fibre (SSMF) PON systems, as presented in Section IV. It is also worth mentioning that, subcarrier grouping has been exploited for conventional OFDM in wireless networks through the proposition of a dual-mode OFDM (DM-OFDM) [14]. In this technique, the grouped subcarriers are modulated by a pair of distinguishable modem-mode constellations. To demodulate the signal, a maximum likelihood (ML) detector and a reduced-complexity near optimal log-likelihood ratio (LLR) detector are employed. Furthermore, dual-mode aided OFDM with constellation power allocation (DM-OFDM-CPA) has also been published [15] where different powers are allocated to different groups of subcarriers enabling each group to be modulated by a different PSK constellation. At the receiver, three detection methods are employed: a low complexity ML detector, an energy-detection (ED), and a LLR detector. Similar to DM-OFDM, DM-OFDM-CPA improves the BER performance significantly compared to OFDM-IM.

TABLE I
EXAMPLE SIPM-SG-OOFDM LOOKUP TABLES FOR n=2, 4, AND 8

| n=2 ($n_H$=1, $n_L$=1) | | n=4 ($n_H$=3, $n_L$=1) | | n=8 ($n_H$=7, $n_L$=1) | |
|---|---|---|---|---|---|
| SG bits | Pattern | SG bits | Pattern | SG bits | Pattern |
| 0 | L H | 00 | H H H L | 000 | H H H H H H H L |
| 1 | H L | 01 | H H L H | 001 | H H H H H H L H |
| | | 10 | H L H H | 010 | H H H H H L H H |
| | | 11 | L H H H | 011 | H H H H L H H H |
| | | | | 100 | H H H L H H H H |
| | | | | 101 | H H L H H H H H |
| | | | | 110 | H L H H H H H H |
| | | | | 111 | L H H H H H H H |

In this paper, subcarrier grouping is first introduced into the newly proposed SIPM-OOFDM technique and its performances are explored, for the first time, in PON transmission systems. In addition, other major contributions of the work presented here are highlighted below: i) exploration and identification of optimum SIPM-SG-OOFDM transceiver design parameters that maximize the signal transmission capacity for arbitrary subcarrier group sizes; ii) proposition and exploration of an effective SG-associated automatic error detection and correction technique with zero-overhead and low DSP complexity. It should also be noted, in particular, that subcarrier grouping can also be applied easily in both SIPM-OOFDM-SPM and ML-SIPM-OOFDM. Since SG-associated operating principles, their DSP implementation procedures and corresponding performance advantages are very similar for these transmission techniques, for simplicity but without losing any generality, in this paper special attention is therefore focused on SIPM-OOFDM only.

## II. OPERATING PRINCIPLE

In general, the operating principles of the proposed SIPM-SG-OOFDM technique are very similar to SIPM-OOFDM [11], except that the SIPM-SG-OOFDM data-encoding (data-decoding) DSP algorithms in the transmitter (receiver) are modified as explained below: in the SIPM-SG-OOFDM transmitter, each symbol consisting of a total number of $N$ subcarriers is split into $G$ groups and each group contains $n$ subcarriers, i.e., $N=nG$. To minimise the DSP complexity, simple predefined lookup tables (LUTs) embedded

in the transceiver map the incoming data sequence to a specific subcarrier power pattern for each subcarrier group, thus enabling extra information bits to be carried in the SG information-bearing dimension. The total number of bits conveyed by the i-th subcarrier group, $B_i$, is formulated as $B_i = B_{1i} + B_{2i}$ with $B_{1i}$ representing the bits carried by the conventional subcarrier information-bearing dimension, and $B_{2i}$ representing the extra bits carried in the SG information-bearing dimension. For the conventional subcarrier information-bearing dimension, $B_{1i}$ is given by

$$B_{1i} = n_{Hi} b_H + n_{Li} b_L \quad (1)$$

where $n_{Hi}$ ($n_{Li}$) are the number of high (low) power subcarriers within the i-th subcarrier group, and satisfy $n = n_{Hi} + n_{Li}$. $b_H$ and $b_L$ are the number of information bits carried by individual high and low power subcarriers, respectively, in the conventional information-bearing domain.

It is well known that, in the SG information-bearing dimension, the total number of bits that can be carried by the i-th subcarrier group, $B_{2i}$, depend on the total number of possible subcarrier power patterns available in the group. $B_{2i}$ can be expressed as

$$B_{2i} = \left\lfloor log_2(C_n^{n_{Hi}}) \right\rfloor, \text{ where } n_{Hi} < n \quad (2)$$

where $C_n^{n_{Hi}}$ denotes the total number of possible subcarrier power patterns and $\lfloor . \rfloor$ denotes the floor function. Clearly, the total number of information-carrying subcarrier power patterns is $2^{B_{2i}}$. When $C_n^{n_{Hi}} = 2^{B_{2i}}$, each possible subcarrier power pattern of the $C_n^{n_{Hi}}$ set can be used to map $B_{2i}$ information bits, whilst when $C_n^{n_{Hi}} > 2^{B_{2i}}$, redundant subcarrier power patterns occur.

Table I illustrates the information-carrying subcarrier power pattern examples for three subcarrier group sizes. For the simplest case of $n$=2, to encode an incoming pseudo-random binary sequence (PRBS) stream, when ''1(0)'' bit is encountered, the corresponding subcarrier power pattern within a given subcarrier group is set high-low (low-high). This enables 1 extra information bit per group carried in the SG information-bearing dimension. On the other hand, in the conventional information-bearing dimension, further 5 bits from the PRBS stream are truncated, of which the first 3(2) are encoded using 8-PSK (QPSK) and the remaining 2(3) are encoded using QPSK (8-PSK).

At the receiver, to determine the received subcarrier power level, the subcarrier power detection and threshold decision DSP functions are employed, which are identical to those reported in [11]. These DSP functions, which are located between the fast Fourier transform (FFT) and channel estimation and equalization, first calculate the optimum power threshold for the subcarrier, by making use of a training sequence that is periodically inserted into the user data sequence in the transmitter. The subcarrier power threshold, $P_{threshold}$, is defined as

$$P_{threshold} = \frac{P_{8\text{-}PSK} + P_{QPSK}}{2} \quad (3)$$

where $P_{8\text{-}PSK}$ and $P_{QPSK}$ are the received powers of the same subcarrier encoded using 8-PSK and QPSK, respectively.

The DSP function of the zero-overhead automatic error correction is described below, and its procedures are illustrated in Fig. 1. By making use of the identified frequency-dependent

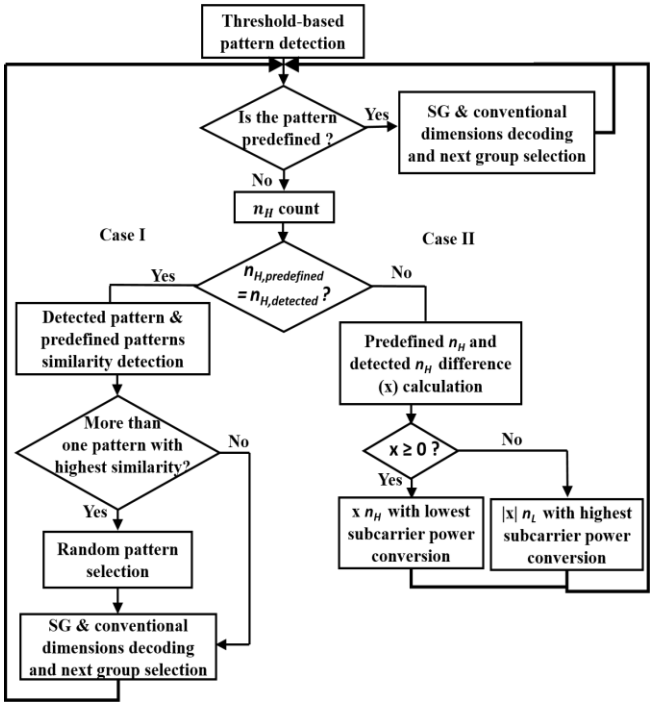

Fig. 1. Zero-overhead automatic error correction procedure adopted in the SIPM-SG-OOFDM receiver.

subcarrier power threshold, the subcarrier power pattern of a targeted subcarrier group is firstly determined, which is then compared with the predefined subcarrier power pattern set stored in the group associated LUT at the receiver. If the detected subcarrier power pattern belongs to the predefined set, then the group-conveyed information bits are decoded accordingly in both the SG information-bearing dimension and the conventional information-bearing dimension. On the other hand, if the detected subcarrier power pattern of the group does not belong to the predefined subcarrier power pattern set, calculations of the total number of high power subcarriers occurring in the group are then performed, based on which two different cases may occur:

- Case I, where the calculated high power subcarrier number matches the adopted value, i.e., the detected subcarrier power pattern is one of the redundant subcarrier power patterns. For specific $n$ and $n_{Hi}$, each individual redundant subcarrier power pattern can be made known easily, together with its similarity with respect to each of the predefined subcarrier power pattern. Here the subcarrier power pattern similarity is defined as the minimum number of necessary subcarrier power status changes required to convert the present subcarrier power pattern to a targeted predefined one. For this case, the predefined subcarrier power pattern with the highest similarity with respect to the detected pattern is selected to replace the detected one; whilst there exist more than one predefined subcarrier power patterns with the same highest similarity with respect to the detected pattern, then a random selection is made from the predefined subcarrier power patterns with the same similarity. Mapping between the detected subcarrier power pattern and the best matching predefined

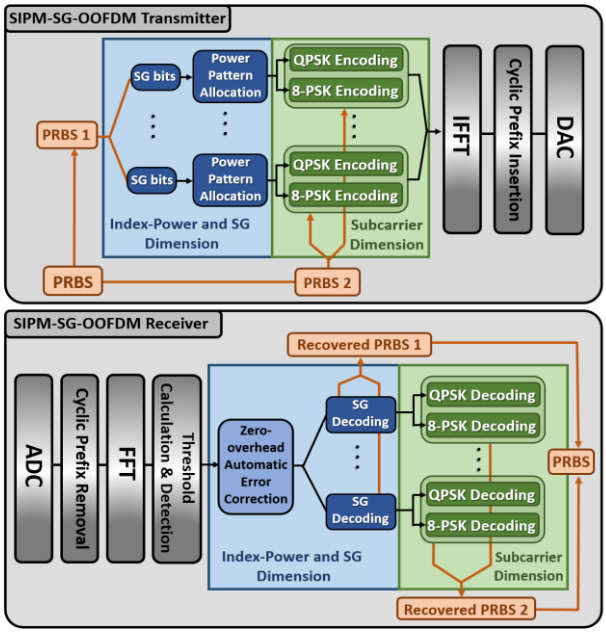


Fig. 2. Schematic illustration of the SIPM-SG-OOFDM transceiver model

subcarrier power pattern can be implemented with simple LUTs.

- Case II, where the calculated number of high power subcarriers of the detected group does not match the adopted value, and their difference is assumed to be x. When $x \geq 0$, x high power subcarriers with lowest subcarrier powers are converted to low power subcarriers; whilst when $x \leq 0$, $|x|$ low power subcarriers with highest subcarrier powers are converted to high power subcarriers. After that, the aforementioned DSP procedures can be applied to process the subcarrier group with converted subcarrier power status. The required DSP for Case II can be implemented with simple logic functions such as comparators, multiplexers and combinational logic, thus the increase in overall receiver DSP complexity is minimal. Furthermore, when comparing complexity to OFDM-based wireless systems involving subcarrier index modulation, low complexity is achieved as the wireless systems [14]-[17] are based on schemes that require complex functions, for example ML detectors (complex multiplications), LLR detectors (multiplications, divisions, logarithms and exponentials) and ED (multiplications and divisions).

Based on above discussions, it is easy to understand the following three points:

- For a specific hardware transceiver design, variations in subcarrier grouping can be easily conducted dynamically in the digital domain. As discussed in Section IV, such operation alters, to some extent, the transceiver performance in terms of both signal transmission capacity and system power budget. This implies that subcarrier grouping can improve the transceiver adaptability and performance flexibility.
- The abovementioned SG-induced performance characteristics can be further enhanced when variations in encoding/decoding schemes are also made in the

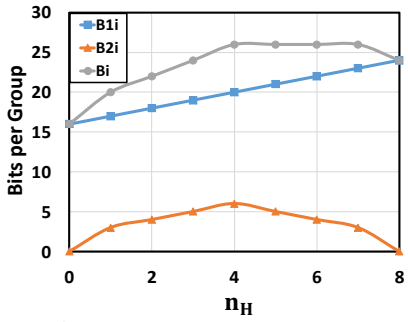


Fig. 3. Number of bits per group versus $n_H$ when N=32, n=8, and G=4

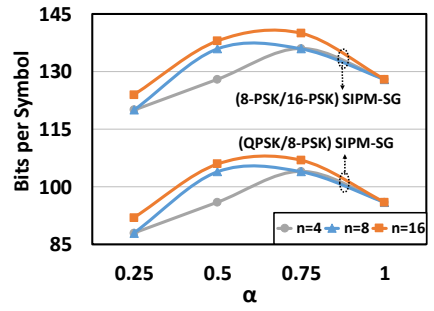


(a)

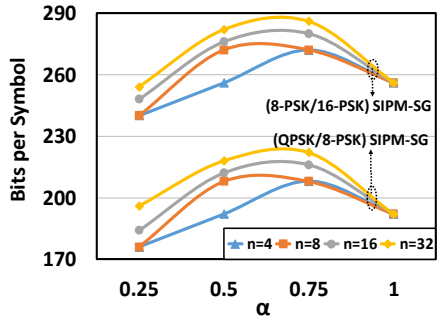


(b)

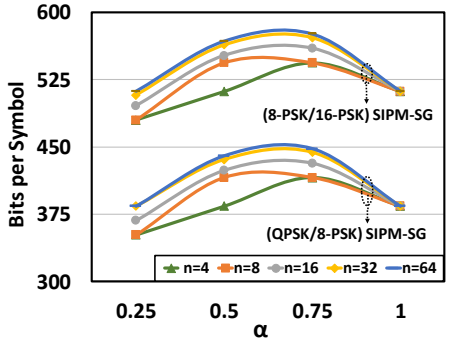


(c)

Fig. 4. Number of bits per symbol versus α for (a) N=32 (b) N=64 (c) N=128.

digital domain, which leads to the transmission technique alterations among SIPM-OOFDM, SIPM-OOFDM-SPM, ML-SIPM-OOFDM and SIPM-SG-OOFDM. Thus it is practically feasible to design a versatile and elastic transceiver capable of dynamically varying its performance characteristics to always provide optimum performances for different system/traffic status.

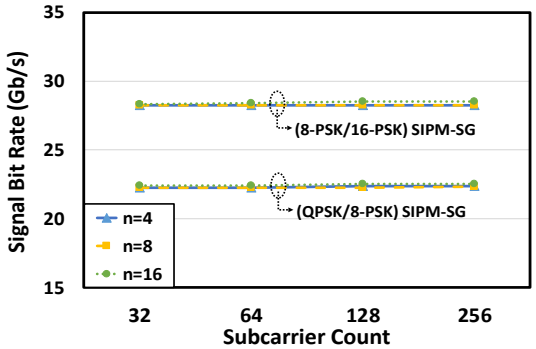


Fig. 5. Signal bit rate performance of both (QPSK/8-PSK) SIPM-SG and (8-PSK/16-PSK) SIPM-SG versus subcarrier count.

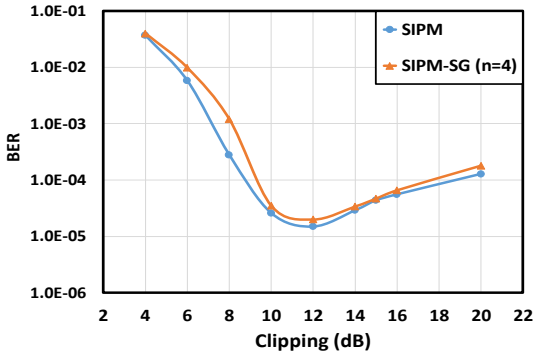


Fig. 6. Overall BER versus clipping ratio over 25km SSMF IM/DD transmission systems with the optical launch power fixed at -9dBm.

TABLE II
TRANSCEIVER AND TRANSMISSION SYSTEM PARAMETERS

| Parameter | Value |
|---|---|
| Total number of IFFT/FFT points | 64 |
| Data-carrying subcarriers | 31 |
| Modulation formats | QPSK or 8-PSK |
| PRBS data sequence length | 400,000 bits |
| Cyclic prefix | 25% |
| DAC & ADC sample rate | 12.5GS/s |
| DAC & ADC bit resolution | 9 bits |
| Clipping ratio | 12 dB |
| PIN detector sensitivity | −19 dBm* |
| PIN responsivity | 0.8A/W |
| SSMF dispersion parameter at 1550 nm | 16 ps/(nm.km) |
| SSMF dispersion slope at 1550 nm | 0.07 ps/nm/nm/km |
| Linear fiber attenuation | 0.2dB/km |
| Kerr coefficient | $2.35 \times 10^{-20}$ m$^2$/W |

*Corresponding to 10Gb/s non-return-to-zero data at a BER of $1.0 \times 10^{-9}$

- Errors do not propagate across different subcarrier groups and different symbols, as each subcarrier group is treated separately in coding/decoding.

To summarize the above-described SIPM-SG-OOFDM operating principle, Fig. 2 is presented, where major subcarrier grouping DSP functions incorporated in the transmitter and receiver are illustrated.

## III. TRANSCEIVER PARAMETER OPTIMIZATION

The main objective of this section is to identify optimum subcarrier grouping parameters capable of maximizing the SIPM-SG-OOFDM transmission capacity. Based on Eq.(1) and Eq.(2), the total number of bits that can be transmitted by the i-th symbol is

$$B_i = \sum_{i=1}^{G} [n_{Hi} b_H + n_{Li} b_L + \lfloor \log_2(C_n^{n_{Hi}}) \rfloor] \quad (4)$$

From Eq.(4), it is easy to understand that $B_{1i}$ reaches its maximum when $n_{Hi} = n$, however, this results in $B_{2i}$=0. On the other hand, $B_{2i}$, is maximised when $n_{Hi} = n/2$, under which $B_{1i}$ can, however, only reach half of its full potential. To explore the information carrying capacity trade-off between these two information-bearing dimensions, the number of information bits carried by each subcarrier group is plotted in Fig. 3 for the following parameters: $N$=32, $n$=8, and $G$=4. Fig. 3 indicates that $B_i$ is maximized at an optimum $n_{Hi}$, termed, $n_{Hopt}$.

To eliminate the impact of subcarrier group size on the performance of different subcarrier grouping schemes, a parameter α is introduced here, which represents the ratio between the total number of high power subcarriers and the total number of subcarriers within a group. Fig. 4 is plotted to investigate the α-dependent information bits per symbol. This figure also investigates the α-impact when higher modulation formats are considered on SIPM-SG-OOFDM such as 8-PSK (16-PSK) as low (high) power encoded subcarriers. It can be seen in Fig. 4(a) that, for different subcarrier group sizes, the maximum information bits per symbol are achieved when α is approximately 0.7. Comparisons between Fig. 4(a), Fig. 4(b) and Fig. 4(c) also indicate that the optimum α remains almost constant regardless of variations in $N$, $n$, and the modulation formats used in SIPM-SG-OOFDM. Thus α =0.7 can be regarded as an optimum grouping parameter, which will be considered in all the following numerical simulations. It is also shown in Fig. 4 that the total number of bits per symbol increases with $n$, this, however, does not affect the overall achievable SIPM-SG-OOFDM transmission capacity as shown in Fig.5 which explores the signal bit rate performance of both QPSK/8-PSK SIPM-SG-OOFDM and 8-PSK/16-PSK SIPM-SG-OOFDM while increasing $N$. For both cases, Fig.5 shows a flat signal bit rate developing trend. More importantly, a 27% increase in signal bit rate is achieved when 8-PSK and 16-PSK are used instead of QPSK and 8-PSK, respectively. For simplicity but without losing any generality, QPSK/8-PSK SIPM-SG-OOFDM is considered in the following parts of this paper.

## IV. SIPM-SG-OOFDM TRANSMISSION PERFORMANCE OVER IM/DD PON SYSTEMS

### A. Signal Transmission Capacity

By making use of the transceiver architecture identical to SIPM-OOFDM [11], the net SIPM-SG-OOFDM signal bit rate, $R$, is given by

$$R = \frac{(\sum_{i=1}^{G-1}(nb_H\alpha + nb_L(1-\alpha_{opt}) + \lfloor log_2(C_n^{n_{Hiopt}}) \rfloor) + \beta) f_s}{2N(1+\sigma)} \quad (5)$$

where $\beta = ((n-1)b_H\alpha + (n-1)b_L(1-\alpha_{opt}) + \lfloor log_2(C_n^{n_{Hopt}}) \rfloor)$ accounts for the information bits conveyed in the final group of a symbol due to 31 data-carrying subcarriers; $f_s$ is the sampling rates of the digital-to-analogue convertor (DAC) and analogue-to-digital convertor (ADC), and $\sigma$ is the coefficient introduced to take into account the signal transmission bit rate reduction due to cyclic prefix and training sequence. In numerical simulations, use is made of the optimum subcarrier grouping parameter identified in Section III and the representative transceiver parameters listed in Table II. As shown in this table, a clipping ratio of 12dB is used which is the

TABLE III
SIGNAL TRANSMISSION BIT RATE COMPARISONS

| Modulation Format | Signal Bit Rate (Gb/s) |
|---|---|
| 8-PSK | 17.80 |
| SIPM | 20.77 |
| SIPM-SG | 23.125 |
| 16-PSK | 23.73 |

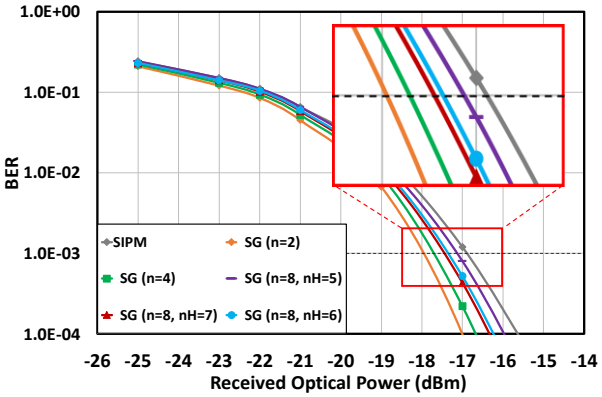


Fig. 7. Overall channel BER versus received optical power after transmitting through 25 km SSMF IM/DD PON systems for SIPM-OOFDM and SIPM-SG-OOFDM for the cases of n=2,4, and 8 ($n_H$=5, 6, and 7).

optimum value for SIPM-OOFDM transceivers identified in [11]. The same value is adopted here as numerical simulation results have shown that SIPM-SG-OOFDM and SIPM-OOFDM have almost identical peak-to-average power ratios (PAPRs). This is also confirmed in Fig.6 which investigates the impact of the clipping ratio on both SIPM-OOFDM and SIPM-SG-OOFDM transmission performance over 25km SSMF IM/DD with an optical launch power of -9dBm. This figure also implies that the clipping ratio is subcarrier grouping-independent. The SIPM-SG-OOFDM signal transmission capacity can be easily computed and compared with other transmission techniques as summarized in Table III. In this table, it is shown that the proposed technique gives rise to a maximum signal transmission bit rate of 23.125Gb/s ($n$=4), which exceeds the 8-PSK-encoded OOFDM and the QPSK/8-PSK-encoded SIPM-OOFDM by approximately 30% and 11%, respectively, and the 8-PSK/QPSK-encoded SIPM-SG-OOFDM transmission capacity is very similar to the 16-PSK/16-QAM-endoded OOFDM transmission capacity, which, however, corresponds to a high minimum received optical power required for achieving a BER of $1.0\times10^{-3}$.

Such an improvement in signal transmission capacity also indicates that based on an identical transceiver architecture, at least >30% variations in signal transmission capacity are achievable by just altering DSP design configuration. In particular, this signal transmission capacity dynamic range can also be further increased when use is made of the adaptive group power loading technique.

### *B. SIPM-SG-OOFDM Transmission Performance Over 25 km SSMF IM/DD PON Systems*

In this subsection, a VPIphotonics SSMF simulation model is used to explore the 23.125Gb/s SIPM-SG-OOFDM transmission performances over 25km SSMF IM/DD PON systems subject to the transceiver/system parameters listed in Table II. The parameters listed in Table II are identical to those reported in [11]. To highlight the transmission performance of the proposed technique, in all numerical simulations an ideal intensity modulator is adopted, which produces an optical field output signal, $S_O(t)$, having a waveform governed by

$$S_O(t) = \sqrt{Se(t)} \qquad (6)$$

where $Se(t)$ is the electrical driving current of the SIPM-SG-OOFDM signal with an optimum dc bias current being added. At the receiver a PIN with a receiver sensitivity of −19 dBm is also employed. Both shot noise and thermal noise are considered, which are simulated utilizing the procedures similar to those presented in [18].

For fixed optical launch powers of -9dBm, Fig. 7 shows the bit error rate (BER) performances of the proposed technique and the previously published SIPM-OOFDM technique. In Fig.7, five subcarrier grouping schemes for $N$=32 are considered, which are: $n$=2 ($n_H$=1), 4 ($n_H$=3), and 8 ($n_H$=5, 6, and 7), each of these $n_H$ values is close to the identified optimum α value for the corresponding $n$ parameter. It is shown in Fig. 7 that, compared with 20.177Gb/s SIPM-OOFDM signal, a maximum OSNR gain of approximately 1.0dB is achieved at an adopted FEC limit of $1.0\times10^{-3}$ for the 23.125Gb/s SIPM-SG-OOFDM signal.

To further explore the relationships between the OSNR gain and various subcarrier grouping schemes, Fig. 8 is plotted, which shows a reduction in OSNR gain with increasing $n$. This is because of the occurrence of an increased redundant pattern status as $n$ increases. As evidenced in Fig. 8, for $n$=8 with various $n_H$ parameters, the lowest OSNR gain is observed when the redundant pattern status are maximum. This indicates that the maximum 1dB OSNR gain is achievable regardless of the

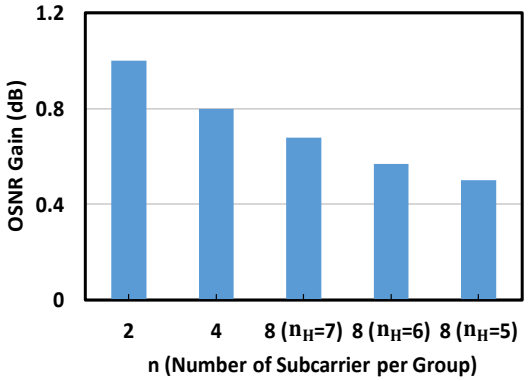


Fig. 8. OSNR gain for the cases of n=2,4, and 8 ($n_H$=5, 6, and 7)

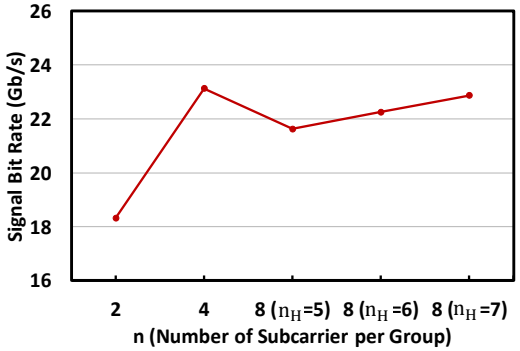


Fig. 9. Signal bit rates for the cases of n=2,4, and 8 ($n_H$=5,6, and 7)

grouping size *n*, as long as necessary improvements are made in the encoder/decoder algorithm procedure. For these five cases, Fig. 9 summarizes their corresponding signal bit rate performances. Fig. 9 shows a slight group size-dependent signal transmission capacity as predicted in [13].

## V. Conclusions

As an improved variant of the previously published SIPM-OOFDM technique, SIPM-SG-OOFDM has been proposed and numerically investigated, for the first time, for signal transmissions over 25km SSMF IM/DD PON systems. Numerical explorations have been undertaken in the optimum SIPM-SG-OOFDM transceiver design and its corresponding maximum achievable transmission performance over the considered PON systems. It has been shown that, compared to SIPM-OOFDM, in addition to an 11% improvement in signal transmission capacity, the proposed technique can also offer an OSNR gain of approximately 1.0dB without significantly increasing the DSP transceiver complexity.

## VI. References


[1] F. Guiomar, S. Amado, R. M. Ferreira, J. Reis, S. M. Rossi, A. Chiuchiarelli, J. Fernandes de Oliveira, A. L. Teixeira, and A. Pinto, "Multicarrier digital backpropagation for 400G optical superchannels," *J. Lightw. Technol.*, vol. 34, no. 8, pp. 1896–1907, Apr. 2016.

[2] F. Li, J. Yu, Z. Cao, J. Zhang, M. Chen, and X. Li, "Experimental demonstration of four-channel WDM 560 Gbit/s 128QAM-DMT using IM/DD for 2-km optical interconnect," J. Lightw. Technol., vol. 35, no. 4, pp. 941–948, Feb. 2017.

[3] Ji Zhou, J. Yu, Q. Cheng, J. Shi, M. Guo, X. Tang, and Y. Qiao, "256-QAM Interleaved Single Carrier FDM for Short-Reach Optical Interconnects," IEEE Photon. Technol. Lett., vol. 29, no. 21, pp. 1796–1799, Nov. 2017.

[4] J. Zhou and Y. Qiao, "Low-PAPR asymmetrically clipped optical OFDM for intensity-modulation/direct-detection systems," IEEE Photon. J., vol. 7, no. 3, Jun. 2015, Art. no. 7101608.

[5] J. Zhou, Y. Yan, Z. Cai, Y. Qiao, and Y. Ji, "A cost-effective and efficient scheme for optical OFDM in short-range IM/DD systems," IEEE Photon. Technol. Lett., vol. 26, no. 13, pp. 1372–1374, Jul. 2014.

[6] C. Li, M. Luo, Z. He, H. Li, J. Xu, S. You and Q. Yang, "Phase noise canceled polarization-insensitive all-optical wavelength conversion of 557-Gb/s PDM-OFDM signal using coherent dual-pump,'' *J. Lightw. Technol.*, vol. 33, no. 13, pp. 2848–2854, Jul. 2015.

[7] C. Guo and L. Dai, " A long reach IM/DD OFDM-PON using super-Nyquist image induced aliasing and code-division multiplexing," *Optical Fibre Commun. (OFC) Conference*, Mar. 2014, Tu2F.3, pp.1–3.

[8] V. Kachhatiya and S. Prince, "Wavelength division multiplexing-dense wavelength division multiplexed passive optical network (WDM-DWDM-PON) for long reach terrain connectivity," *Communication and Sig. Proc. (ICCSP) Conference*, Apr. 2016.

[9] R. Abu-alhiga and H. Haas, "Subcarrier-index modulation OFDM," *Proc. IEEE Int. Sym. Personal, Indoor Mobile Radio Commun.*, Sep. 2009, pp. 177–181.

[10] E. Başar, Ü. Aygölü, E. Panayırcı, and H. Vincent Poor,"Orthogonal frequency division multiplexing with index modulation," *IEEE Trans. Signal Process.*, vol. 61, no. 22, pp. 5536–5549, Nov. 2013.

[11] F. Halabi, L. Chen, S. Parre, S. Barthomeuf, R. P. Giddings, C. Aupetit-Berthelemot, A. Hamié and J. M. Tang, "Subcarrier index-power modulated optical OFDM and its performance in IMDD PON systems," *J. Lightw. Technol.*, vol. 34, no. 9, pp. 2228–2234, May 2016.

[12] L. Chen, F. Halabi, R. P. Giddings, and J. M. Tang, "Subcarrier index-power modulated optical OFDM with superposition multiplexing for IMDD transmission systems," *J. Lightw. Technol*., vol. 34, no. 9, pp. 2228–2234, Oct. 2016.

[13] F. Halabi, L. Chen, R. P. Giddings, A. Hamié and J. M. Tang, "Multilevel subcarrier index-power modulated optical OFDM with adaptive bit loading for IMDD PON systems," *IEEE Photon. J.*, vol. 8, no. 6, Dec 2016.

[14] T. Mao, Z. Wang, Q. Wang, S. Chen, and L. Hanzo, "Dual-mode index modulation aided OFDM," IEEE Access, vol. 5, pp. 50–60, 2017.

[15] X. Zhang, H. Bie, Q. Ye, C. Lei, X. Tang, "Dual-Mode Index Modulation Aided OFDM With Constellation Power Allocation and Low-Complexity Detector Design", IEEE Access, vol. 5, pp. 23871-23880, 2017.

[16] S. Dang, J. P. Coon, and G. Chen, "Adaptive OFDM With Index Modulation for Two-Hop Relay-Assisted Networks," *IEEE Trans. Wirel. Commun.*, vol. 17, no. 3, pp. 1923–1936, Mar. 2018.

[17] R. Fan, Y. J. Yu, and Y. L. Guan, "Generalization of Orthogonal Frequency Division Multiplexing With Index Modulation," *IEEE Trans. Wirel. Commun.*, vol. 14, no. 10, pp. 5350–5359, Oct. 2015.

[18] G. P. Agrawal, *Fibre-Optic Communication Systems*, 2nd ed. Hoboken, NJ, USA: Wiley, 1997.